Journal of
Ceramic Science
and Technology

J. Ceram. Sci. Technol., **08** [2] 255-258 (2017)
DOI: 10.4416/JCST2016-00116
available online at: http://www.ceramic-science.com

Particle Size Effect on the Electrical Properties of Spark-Plasma-Sintered Relaxor Potassium Sodium Niobate Ceramic

C. Wang*[1], J. Chen[1], L. Shen[1], J. Rui[1], X. Yang[1], M. Zhu[2], Y. Hou[2]

[1]Logistics School, Beijing Wuzi University, Beijing 101149, P. R. China
[2]Key Laboratory of Advanced Functional Materials of China Education Ministry, Beijing University of Technology, Beijing 100124, P. R. China

received December 11, 2016; received in revised form Febuary 2, 2017; accepted March 13, 2017

Abstract

30-nm-grain-sized potassium sodium niobate ($(K_{0.5}Na_{0.5})NbO_3$ (KNN)) powders were obtained with the sol-gel method. From these powders as starting materials, high-density KNN ceramics with a relative density of 98.9 % and grain size of 500 nm were prepared with the spark plasma sintering (SPS) method. The processing parameters were a sintering temperature of 900 °C, sintering pressure of 30 MPa and sintering time of 3 min. The phase composition, microstructure and electrical properties of the ceramics have been investigated. The results show that, unlike common micro-grained ceramics, submicron-grained ceramics prepared with the SPS method show obvious dielectric relaxation (dispersion factor γ is 1.31). Meanwhile, the KNN ceramics exhibit good electrical properties such as dielectric constant ε_r = 753, piezoelectric constant d_{33} = 142 pC/N and electromechanical coupling factor k_p = 0.41.

Keywords: Lead-free piezoelectric ceramics, potassium sodium niobate, submicron-grained, dielectric relaxation, electrical properties.

I. Introduction

In recent years, in lead-free piezoelectric ceramic systems, $(K_{0.5}Na_{0.5})NbO_3$ (KNN)-based ceramics have gained most attention and are considered a candidate material for Pb-free piezoelectric material [1–3]. However, it is hard to obtain high-density KNN-based ceramics with the conventional method owing to the volatility of potassium and lack of sintering properties. Usually, KNN powders are prepared based on a solid-state reaction. In this case, the starting materials are oxides or carbonates of Na, K and Nb with grain sizes in the micrometer or submicrometer range. Therefore, a perovskite-phase-forming temperature of 850 °C and above is needed. Further, a higher sintering temperature is needed and it causes unfavorable results, such as severe agglomeration and the volatility of potassium [4–6]. In comparison, nanocrystalline powder has a higher inherent surface area, which provides significantly higher stored energy for solid-state densification, and ultimately results in a lower sintering temperature and higher densification [7,8]. Moreover, this is beneficial for minimizing the potassium loss problem at a lower sintering temperature.

The sol-gel method has been widely used to obtain single-phase nanocrystalline powder [9–11]. In contrast with other methods, the sol-gel process has shown considerable advantages, such as lower crystallization temperature, compositional homogeneity and excellent chemical stoichiometry owing to the mixing of liquid precursors on molecular level. On the other hand, spark plasma sintering (SPS) has been widely used to obtain high-density nanocrystalline ceramics because of the rapid heating rate and short soaking time [12–14].

In our previous work, from KNN nanopowders obtained with the novel sol-gel method, KNN ceramics with grain size of 40 nm were prepared with a spark plasma sintering method. However, the nanocrystalline ceramics showed very weak piezoelectric properties because of the size effect [15]. In this work, by prolonging the sintering time in SPS, KNN ceramics with grain size of 500 nm and relaxor properties are obtained, furthermore their electrical properties are also investigated.

II. Experimental

In this work, the raw materials were niobium oxide (Nb_2O_5, 99.9 %), potassium hydroxide (KOH, 97 %), sodium carbonate (Na_2CO_3, 99.8 %), potassium carbonate (K_2CO_3, 99 %), acetic acid (CH_3COOH, 99.5 %), oxalic acid ($(COOH)_2{\cdot}2H_2O$, 99.5 %), citric acid ($C_6H_8O_7{\cdot}H_2O$, 99.5 %) and nitric acid (HNO_3, 65.0–68.0 %).

KNN nanopowders were prepared with the novel sol-gel method as reported in our previous work [16]. The processing parameters are a heating rate of 20 K/min, calcining temperature of 500 °C and calcining time of 5 h. SPS was performed using the model SPS-3.20 MK-V (Sumitomo Coal Mining Co. Ltd., Japan). The synthesized KNN powders were charged into a SPS graphite die measuring 20 mm in diameter. The temperature was raised to 900 °C and kept for 3 min, under a constant pressure of 30 MPa along the Z-axis. Because of the reducing atmosphere and diffusion of carbon from the die materials, the

* Corresponding author: wancha1981@163.com

sintered samples lost oxygen stoichiometry and their color is black. Then the sintered samples need annealing treatment at 800 °C for 2 h for maintaining oxygen stoichiometry and driving away carbon from the graphite die during sintering.

Transmission electron microscopy (TEM) and selected area electron diffraction (SAED) were performed using a JEM-2000 TEM (JEOL, Tokyo, Japan) to determine the morphology and structure of the KNN nanopowders. To check the densification of ceramics, the apparent density of the KNN ceramics was measured with the Archimedes method using distilled water as a medium. X-ray diffraction (XRD) analysis was performed in θ-2θ mode using a Bruker D8 Advance X-ray diffractometer with CuKα radiation to examine the phase structure. The morphology of the KNN ceramics was observed using a Hitachi model S-3500N scanning electron microscopy (SEM). The obtained ceramics were lapped and electroded with silver paste for electrical property measurements. The dielectric measurements were conducted with an Agilent 4284A precision LCR meter. The ferroelectric hysteresis loops were measured at room temperature with a AixACCT-TF2000 ferroelectric tester. Prior to testing piezoelectric properties, the electroded KNN ceramics were poled in a silicone oil bath at 150 °C by applying a dc field of 4 kV/mm for 30 min and aged for 24 h. The piezoelectric coefficient d_{33} was measured using a ZJ-3D quasi-static piezoelectric d_{33} meter. The electromechanical coupling factor k_p was estimated with the resonance and anti-resonance technique using an Agilent 4294A impedance analyzer.

III. Results and Discussion

Fig. 1 presents a TEM image and SAED pattern of KNN nanopowders prepared with the novel sol-gel method. The image clearly shows that the products were free of hard agglomeration, consisting of a large amount of uniform nano-sized cubic structures with an average size of about 30 nm. The inset of Fig. 1 shows the SAED pattern of a typical individual cube of KNN. The sharp diffraction spots indicate the formation of well-developed, single-crystalline KNN, and the diffraction spots could be indexed well with the orthorhombic perovskite structure of KNN. The three diffraction spots indicated in SAED pattern correspond to (0 1 0), (1 1 1) and (1 0 1), respectively.

The apparent density of the sintered KNN samples was measured to check the densification. The results show that the density is 4.42 g/cm^3, which is 98.9 % of the theoretical density. The SEM images of KNN samples sintered with the SPS method is shown in Fig. 2. It can be seen from Fig. 2 that the KNN sample is very dense, almost no visible pores could be found in it, and the grain size is about 500 nm. Although the SPS temperature is as low as 900 °C, which is more than 200 °C lower than that for the conventional method [4–6], the high-density KNN ceramics can be prepared because the powder densification process is conducted at a low temperature and in a very short time by means of SPS.

Fig. 3 shows the XRD patterns and Rietveld refinement profile of KNN samples sintered by means of the SPS method. The tick marks below the histogram give the positions of all possible Bragg reflections. The difference between the observed and the calculated data is plotted below the tick marks. As shown in Fig. 3, good agreement exists between the calculated and the observed diffraction profiles. The lattice constants of submicron-grained KNN ceramics are refined and the results shows that the structure belongs to orthorhombic symmetry, with a = 0.5627(0) nm, b = 0.3937(9) nm, c = 0.5654(3) nm.

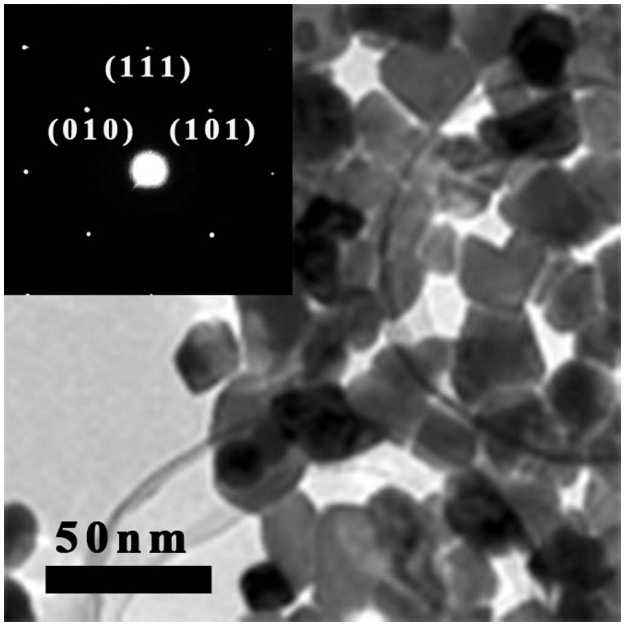

Fig. 1: TEM image of KNN nanopowders. Inset: the SAED pattern of a typical KNN particle.

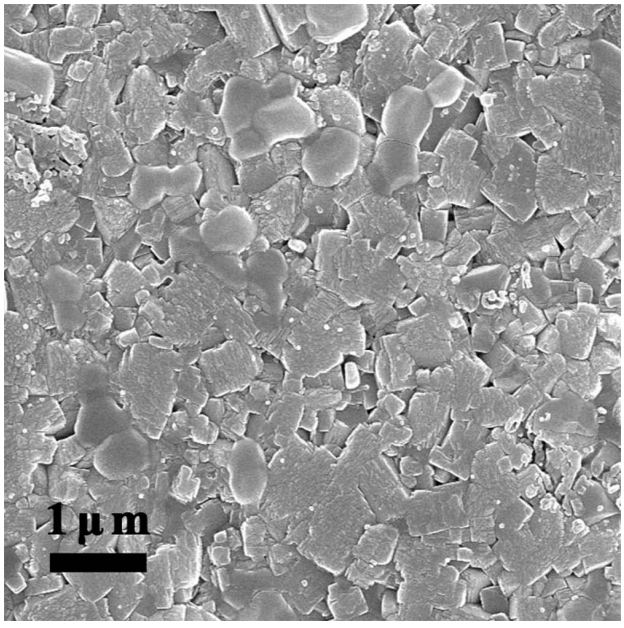

Fig. 2: SEM images of KNN samples sintered with the SPS method.

Fig. 4 shows the temperature dependence of the dielectric constant of KNN ceramics sintered with the SPS method. It can be seen in Fig. 4 that phase transitions are observed at about 200 and 410 °C, corresponding to the phase transitions of orthorhombic-tetragonal and tetragonal-cubic, respectively. The results are similar to the observation in the literature [2]. The dielectric constant ε_r at room temperature is 753, which is much higher than that of pure

KNN ceramics prepared with the conventional method (about 400) [6]. The high density of KNN ceramics can give a reason for the higher dielectric constant. It can also be seen from Fig. 4 that the broadening peak of the dielectric constant near Curie temperature indicates that submicron-grained KNN ceramics show obvious dielectric relaxation. This phenomenon is different from KNN ceramics prepared with the conventional method. For relaxor ferroelectrics, the changes of the dielectric constant near the Curie temperature follow the Uchino-Nomura equation [17]:

$$\frac{1}{\varepsilon_r} - \frac{1}{\varepsilon_{r,max}} = \frac{(T - T_{max})^{\gamma}}{C} \quad (1)$$

where T_{max} denotes the Curie temperature, $\varepsilon_{r,\,max}$ is the dielectric constant at Curie temperature, C is a constant and dispersion factor $\gamma = 1$ for a classical Curie-Weiss ferroelectric, $\gamma = 2$ for a system with a completely diffused transition, and $1 < \gamma < 2$ for systems showing intermediate degrees of diffuseness. To determine the diffuseness of the submicron-grained KNN ceramics sintered with the SPS method, $\ln(1/\varepsilon_r - 1/\varepsilon_{r,\,max})$ as a function of $\ln(T - T_{max})$ and fitting lines are shown in the inset of Fig. 4. It can be seen that the γ of submicron-grained KNN samples in our work is 1.31, which is smaller than that of the 40-nm-grain-sized KNN ceramics ($\gamma = 1.60$) [15]. The diffuse phase transition phenomenon in the normal ferroelectric systems caused by grain size effect has been reported in several articles [18, 19]. When the grain size is reduced, the sensitivity of the Curie temperature depending on the grain size increases considerably, that is small changes in the grain size will cause distribution in the Curie temperature. Usually, the grain size of ceramics is in a certain range, so the submicron-grained KNN ceramics have obvious relaxation ferroelectric characteristics, and this influence is much higher in nano KNN ceramics.

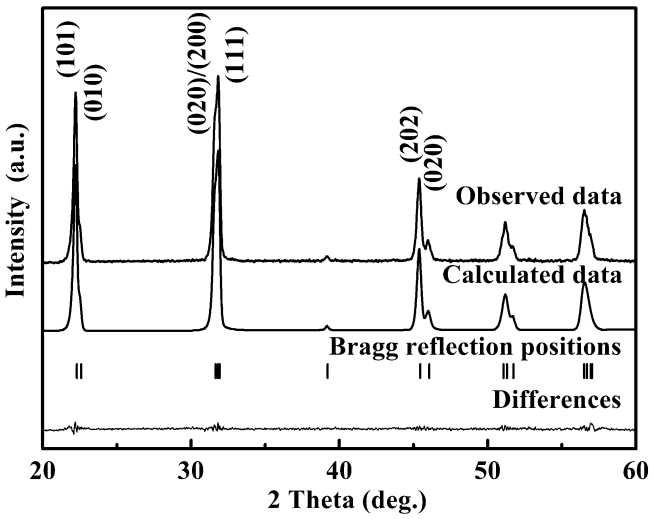

Fig. 3: XRD patterns and Rietveld refinement profile of KNN samples sintered with the SPS method..

A well-saturated ferroelectric hysteresis loop of submicron-grained KNN ceramics derived from nanopowders is shown in Fig. 5. The remanent polarization P_r and the coercive field E_c are 20.4 μC/cm² and 14.6 kV/cm, respectively, which are higher than KNN ceramics prepared with the conventional method [20]. This result indicates that submicron-grained KNN ceramics with a very homogeneous and compact structure derived from nanopowders are effective in obtaining high-resistance specimens under a high electric field, which is favorable for the improvement of piezoelectric properties. In our research, the submicron-grained KNN ceramics derived from nanopowders also show good piezoelectric properties such as d_{33} = 142 pC/N and $k_p = 0.41$.

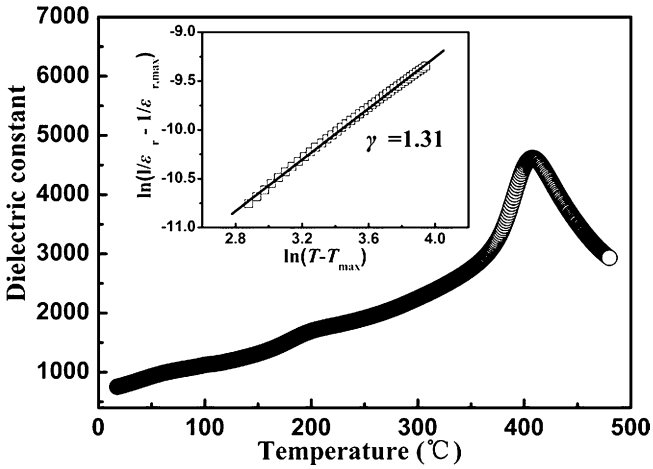

Fig. 4: Temperature dependence of the dielectric constant of KNN ceramics sintered with the SPS method. Inset: $\ln(1/\varepsilon_r - 1/\varepsilon_{r,\,max})$ as a function of $\ln(T - T_{max})$ and fitting lines.

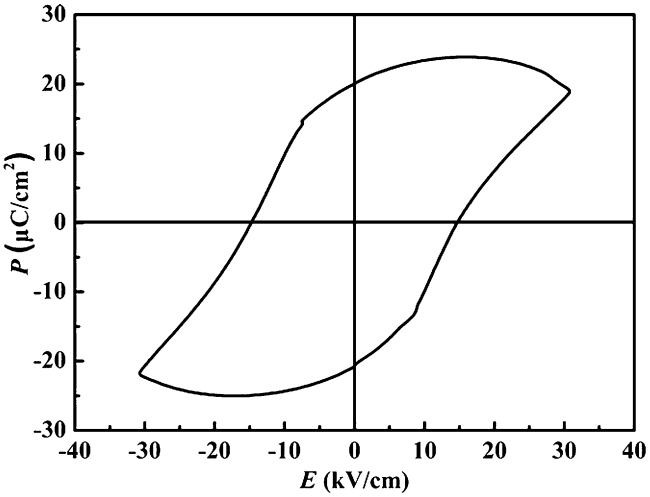

Fig. 5: Ferroelectric hysteresis loop of KNN ceramics sintered with the SPS method.

IV. Conclusions

In this work, 30-nm-grain-sized KNN powders were obtained with the sol-gel method. From these powders as starting materials, KNN ceramics with relative density of 98.9 % and grain size of 500 nm were prepared with the spark plasma sintering (SPS) method. The sintering temperature was 900 °C, sintering pressure was 30 MPa and sintering time was 3 min. The phase composition, microstructure and electrical properties of the ceramics have been investigated. The results show that, unlike common micro-grain ceramics, submicron-grained ceramics prepared with the SPS method show obvious dielectric re-

laxation (dispersion factor γ is 1.31). The small grain size changes caused distribution in the Curie temperature can provide a reason for this special phenomenon. Moreover, because of their fine grain size and high density, the submicron-grained ceramics prepared with the SPS method also exhibit good electrical properties such as $\varepsilon_r = 753$, $d_{33} = 142$ pC/N and $k_p = 0.41$.

Acknowledgement

This work was funded by Youth Scientific Research Fund Project of Beijing Wuzi University (2016XJQN06) and the Project of New Star of Science and Technology of Beijing (Grant no. 2013028).

References

1 Saito, Y., Takao, H., Tani, T., Nonoyama, T., Takatori, K., Homma, T., Nagaya, T., Nakamura, M.: Lead-free piezoceramics, *Nature*, **432**, 84 – 87, (2004).

2 Guo, Y.P., Kakimoto, K., Ohsato, H.: Phase transitional behavior and piezoelectric properties of $Na_{0.5}K_{0.5}NbO_3$ – $LiNbO_3$ ceramics, *Appl. Phys. Lett.*, **85**, 4121 – 4123, (2004).

3 Wu, J.G., Zhang, B.Y., Wu, W.J.: Phase structure and electrical properties of barium-modified potassium-sodium niobate-based lead-free ceramics, *J. Alloy. Compd.*, **651**. 302 – 307, (2015).

4 Cheng, X.J., Gou, Q., Wu, J.G., Wang, X.P., Zhang, B.Y., Xiao, D.Q., Zhu, J.G., Wang, X.J., Lou, X.J.: Dielectric, ferroelectric, and piezoelectric properties in potassium sodium niobate ceramics with rhombohedral-orthorhombic and orthorhombic-tetragonal phase boundaries, *Ceram. Int.*, **40**, 5771 – 5779, (2014).

5 Lee, I.H., Lee, H.S., Kim, Y.H., Gil, S.K., Kang, D.H.: Effects of Al_2O_3 on the ferroelectric properties of sodium potassium lithium niobate lead-free piezoceramics, *Ceram. Int.*, **39**, S709 – S713, (2013).

6 Maeder, M., Damjanovic, D., Setter, N.: Lead-free piezoelectric materials, *J. Electroceram.*, **13**, 385 – 392, (2004).

7 Hou, Y.D., Zhu, M.K., Hou, L., Liu, J. B., Tang, J. L., Wang, H., Yan, H.: Synthesis and characterization of lead-free $K_{0.5}Bi_{0.5}TiO_3$ ferroelectrics by sol-gel technique, *J. Cryst. Growth*, **273**, 500 – 503, (2005).

8 Li, Y.M., Liu, H., Shen, Z.Y., Wang, Z.M., Hong, Y., Li, Y.Y.: Preparation of (K, Na)NbO_3-based lead-free piezoelectric ceramic by microwave-hydrothermal method, *J. Chin. Ceram. Soc.*, **39**, 1922 – 1927, (2011).

9 Predoana, L., Barau, A., Zaharescu, M., Vassilchina, H., Velinova, N., Banov, B., Momchilov, A.: Electrochemical properties of the $LiCoO_2$ powder obtained by sol-gel method, *J. Eur. Ceram. Soc.*, **27**, 1137 – 1142, (2007).

10 Linardos, S., Zhang, Q., Alcock, J.R.: Preparation of sub-micron PZT particles with the sol-gel technique, *J. Eur. Ceram. Soc.*, **26**, 117 – 123, (2006).

11 Krebs, J.K., Happek, U.: Optical spectroscopy of trivalent chromium in sol-gel lithium niobate, *Appl. Phys. Lett.*, **87**, 251910 – 1 – 3, (2005).

12 Li, B.R., Liu, D.Y., Liu, J.J.: Two-step sintering assisted consolidation of bulk titania nano-ceramics by spark plasma sintering, *Ceram. Int.*, **38**, 3693 – 3699, (2012).

13 Kumar, R., Chaubey, A.K., Bathula, S.: Synthesis and characterization of Al_2O_3-TiC nano-composite by spark plasma sintering, *Int. J. Refract. Met. H.*, **54**, 304 – 308, (2016).

14 Nuthalapati, M., Karak, S.K., Chakravarty D.: Development of nano-Y_2O_3 dispersed zr alloys by mechanical alloying and spark plasma sintering, *Mater. Sci. Eng. A*, **650**, 145 – 153, (2016).

15 Wang, C., Chen, J., Chen H.L., Hou, Y.D., Zhu, M.K.: Preparation and properties of nanocrystalline potassium sodium niobate ceramics, *J. Inorg. Mater.*, **30**, 59 – 64, (2015).

16 Wang, C., Hou, Y.D., Ge, H., Y., Zhu, M.K., Wang, H., Yan, H.: Sol-gel synthesis and characterization of lead-free LNKN nanocrystalline powder, *J. Cryst. Growth*, **310**, 4635 – 4639, (2008).

17 Uchino, K., Nomura, S.: Critical exponents of the dielectric constants in diffused-phase-transition crystals, *Ferroelectrics*, **44**, 55 – 61, (1982).

18 Chattopadhyay, S., Ayyub, P., Palkar, V.R., Multani, M.: Size-induced diffuse phase transition in the nanocrystalline ferroelectric $PbTiO_3$, *Phys. Rev. B*, **52**, 13177 – 13183, (1995).

19 Park, Y., Lee, W.J., Kim, H.G.: Particle-size-induced diffuse phase transition in the fine-particle barium titanate porcelains, *J. Phys. Condens. Mat.*, **9**, 9445 – 9456, (1997).

20 Zhang, L.M., Zhang, B.P., Li, J.F., Wang, K., Zhang, H.L.: Normal sintering of lead-free piezoceramic potassium sodium niobate and its electrical properties, *J. Chin. Ceram. Soc.*, **35**, 1 – 5, (2007).